Convective Heat Transfer Performance of Nanofluid in a Horizontal Annular Duct Considering Nanoparticles Shapes Effect

Conference Paper · November 2019

DOI: 10.1109/IRSEC48032.2019.9078326

2 authors:

Benkhedda Mohamed
University M'Hamed Bougara of Boumerdes
9 PUBLICATIONS **27** CITATIONS

SEE PROFILE

Toufik Boufendi
University of Constantine 1
17 PUBLICATIONS **61** CITATIONS

SEE PROFILE

Convective Heat Transfer Performance of Nanofluid in a Horizontal Annular Duct Considering Nanoparticles Shapes Effect

Mohamed Benkhedda[ab]*
[a] Faculty of Sciences, M'Hamed Bougara University
Boumerdes, Algeria
(*) m.benkhedda@univ-boumerdes.dz

Toufik Boufendi [b]
[b] Energy Physics Laboratory, Faculty of Science,
Brothers Mentouri University Constantine 1,
Constantine, Algeria

Abstract— **In The present study investigates laminar forced convection heat transfer in a concentric annular space saturated with nanofluids. The inner cylinder is adiabatic while the outer cylinder is uniformly heated. The governing equations with the appropriate boundary conditions are discretized by the finite volume method with second order precision and solved by using the SIMPLER and Thomas algorithms. The effects of some parameters such as the nanoparticles types Ag and CuO, the shapes like blades, platelets, cylinder and bricks, and nanofluid volume fraction on heat transfer are completely studied and discussed. The results show that the Nusselt number, the bulk, and wall temperatures increase with the increase of nanoparticle volume fraction. A linear increase is observed for the average Nusselt number by increasing the volume fraction. Silver nanoparticles Ag give better heat transfer compared with the CuO nanoparticles for the blade shape followed by the elongated shape like platelet and cylinder and in last place brick shape.**

Keywords- nanoparticle shape; annular duct; forced convection; nanofluid; numerical study.

I. INTRODUCTION

Nanofluid is a suspension of nanometer-sized particles (<100 nm), such as and in the base fluid such as water, ethylene glycol (EG), and oil. This new fluid can improve the performance of heat transfer systems in many industrial applications such as engine cooling, nuclear cooling system, refrigeration, solar cells, food drying, chemical processes, power generation, and biomedical. This new fluid was termed the first time a "Nanofluid" by Choi [1] in 1995 at the Argonne National Laboratory to characterize the new class of fluids with superior thermal properties to prevalent base fluids. The improvement of the thermal conductivity of the nanofluid depends on several parameters such as volume fraction, type of material, temperature and shape. Several studies were made to see the influences of these parameters on the thermophysical properties especially for improving the thermal conductivity. The use of nanofluids as a new technique for reaching a higher heat transfer was introduced by Eastman et al. [2]. The theoretical thermal conductivity model that considers the shape of the nanoparticle [3]. The model of thermal conductivity considering spherical nanoparticle shape presented by Maxwell [4]. The heat transfer of the nanofluid into the horizontal annular concentric cylinder is a particularly interesting problem. Izadi et al [5] numerically studied laminar forced convection in the annulus of nanofluid containing Al2O3 nanoparticles dispersed in water base fluid. It shows the dimensionless axial velocity profile does not affect with nanoparticle volume fraction, while the bulk temperature increase by increasing volume fraction. The friction coefficient does not change in the region fully developed. Mokhtari et al. [6] studied numerical laminar mixed convection in horizontal annuli it is observed that the local Nusselt number increases with an increase in nanoparticle volume fraction, Grashof number, and radius ratio. Benkhedda et al.[7] analyzed mixed convection in a horizontal annulus with a heated outer cylinder. They reported that the effects of nanoparticle concentration on nanofluid and wall temperatures are very significant. Also, Benkhedda et al [8] numerically studies of hybrid nanofluid (Ag-TiO_2/water) compared to its nanofluid (Ag/water) and the water base fluid, they found that the mixed convection heat transfer using the hybrid nanofluid is better than the nanofluid and pure water.

Following this rich evolution of the nanofluids field, our contribution to the present work is the numerical simulation of three-dimensional laminar forced convection in annuli filled by two different nanofluids. Single phase approach is adopted. This study has focused on different volume fraction, two types Ag and CuO and different shapes like a blade, platelet, cylinder, and brick of nanoparticles related to thermal and hydrodynamic effects on fully developed flow through the annulus. The Reynolds number is fixed at 800 and results have been compared and discussed in terms of velocity, bulk and wall temperatures profiles, and Nusselt number.

II. MATHEMATICAL FORMULATION

Fig. 1 shows the schematic of the considered physical model. It consists of two horizontal concentric cylinders, with outer and inner diameters equal to 10 and 5 mm, respectively, and the length is of 1000 mm, is illustrated in. The radius ratio is fixed to 2 ($r_o/r_i=2$). The outer cylinder is maintained at a constant heat flux while the inner cylinder is adiabatic. The nanofluid is assumed Newtonian with neglecting of the viscous

978-1-7281-5152-6/19/$31.00 ©2019 IEEE

dissipation and pressure work. In addition, the Boussinesq approximation is applicable and ultrafine solid particles have been considered, single phase homogeneous model (SPM) is applied. The governing equations for natural convection flow using conservation of mass, momentum and energy equations can be written in dimensionless form as follows:

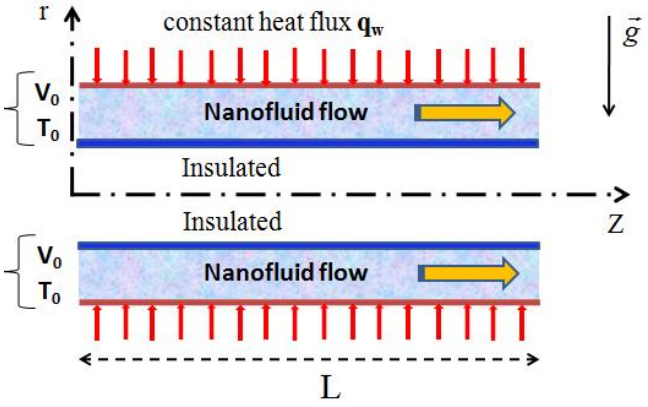

Figure 1. Schematic diagram of the annular duct.

A. Continuity equation:

$$\frac{1}{r^*}\frac{\partial\left(r^* u^*\right)}{\partial r^*}+\frac{1}{r^*}\frac{\partial w^*}{\partial\theta}+\frac{\partial v^*}{\partial z^*}=0 \tag{1}$$

B. Radial momentum equation:

$$\frac{\partial u^*}{\partial t^*}+\frac{1}{r^*}\frac{\partial}{\partial r^*}\left(r^* u^* u^*\right)+\frac{1}{r^*}\frac{\partial}{\partial\theta}\left(u^* w^*\right)+\frac{\partial}{\partial z^*}\left(v^* u^*\right)$$
$$-\frac{w^{*2}}{r^*}=-\frac{\partial p^*}{\partial r^*}+ \tag{2}$$
$$\frac{1}{\mathrm{Re}}\times\frac{\left(\frac{\mu_{nf}}{\mu_f}\right)}{\left(\frac{\rho_{nf}}{\rho_f}\right)}\left[\frac{1}{r^*}\frac{\partial}{\partial r^*}\left(r^*\frac{\partial u^*}{\partial r^*}\right)+\frac{1}{r^{*2}}\frac{\partial}{\partial\theta}\left(\frac{\partial u^*}{\partial\theta}\right)+\frac{\partial}{\partial z^*}\left(\frac{\partial u^*}{\partial z^*}\right)-\frac{u^*}{r^{*2}}-\frac{2}{r^{*2}}\frac{\partial w^*}{\partial\theta}\right]$$

C. Angular Momentum Equation:

$$\frac{\partial u^*}{\partial t^*}+\frac{1}{r^*}\frac{\partial}{\partial r^*}\left(r^* u^* w^*\right)+\frac{1}{r^*}\frac{\partial}{\partial\theta}\left(w^* w^*\right)+\frac{\partial}{\partial z^*}\left(v^* w^*\right)$$
$$-\frac{w^{*2}}{r^*}=-\frac{1}{r^*}\frac{\partial p^*}{\partial\theta}+ \tag{3}$$
$$\frac{1}{\mathrm{Re}}\times\frac{\left(\frac{\mu_{nf}}{\mu_f}\right)}{\left(\frac{\rho_{nf}}{\rho_f}\right)}\left[\frac{1}{r^*}\frac{\partial}{\partial r^*}\left(r^*\frac{\partial w^*}{\partial r^*}\right)+\frac{1}{r^{*2}}\frac{\partial}{\partial\theta}\left(\frac{\partial w^*}{\partial\theta}\right)+\frac{\partial}{\partial z^*}\left(\frac{\partial w^*}{\partial z^*}\right)-\frac{w^*}{r^{*2}}-\frac{2}{r^{*2}}\frac{\partial u^*}{\partial\theta}\right]$$

D. Axial Momentum Equation:

$$\frac{\partial u^*}{\partial t^*}+\frac{1}{r^*}\frac{\partial\left(r^* u^* v^*\right)}{\partial r^*}+\frac{1}{r^*}\frac{\partial}{\partial\theta}\left(w^* v^*\right)+\frac{\partial}{\partial z^*}\left(v^* v^*\right)-\frac{w^{*2}}{r^*}$$
$$=-\frac{\partial p^*}{\partial z^*}+\frac{1}{\mathrm{Re}}\frac{\left(\frac{\mu_{nf}}{\mu_f}\right)}{\left(\frac{\rho_{nf}}{\rho_f}\right)}\left[\frac{1}{r^*}\frac{\partial}{\partial r^*}\left(r^*\frac{\partial v^*}{\partial r^*}\right)+\frac{1}{r^{*2}}\frac{\partial}{\partial\theta}\left(\frac{\partial v^*}{\partial\theta}\right)+\frac{\partial}{\partial z^*}\left(\frac{\partial v^*}{\partial z^*}\right)\right] \tag{4}$$

E. Energy Equation:

$$\frac{\partial T^*}{\partial t^*}+\frac{1}{r^*}\frac{\partial}{\partial r^*}\left(r^* u^* T^*\right)+\frac{1}{r^*}\frac{\partial}{\partial\theta}\left(w^* T^*\right)+\frac{\partial}{\partial z^*}\left(v^* T^*\right)=$$
$$\frac{1}{\mathrm{Re.Pr}}\times\frac{\left(\frac{\mathrm{k_{nf}}}{\mathrm{k_f}}\right)}{\left(\frac{(\rho C_p)_{\mathrm{nf}}}{(\rho C_p)_{\mathrm{f}}}\right)}\left[\frac{1}{r^*}\frac{\partial}{\partial r^*}\left(r^*\frac{\partial T^*}{\partial r^*}\right)+\frac{1}{r^{*2}}\frac{\partial}{\partial\theta}\left(\frac{\partial T^*}{\partial\theta}\right)+\frac{\partial}{\partial z^*}\frac{\partial T^*}{\partial z^*}\right] \tag{5}$$

F. The Boundary Conditions:

$$\text{At } r^*=0.5:\quad u^*=w^*=v^*=0,\quad \frac{\partial T^*}{\partial r^*}=0 \tag{6}$$

$$\text{At } r^*=1:\quad u^*=w^*=v^*=0,\quad \frac{\partial T^*}{\partial r^*}=1 \tag{7}$$

$$\text{At } Z^*=0:\quad u^*=w^*=0\ ,\quad v^*=1,\ T^*=0 \tag{8}$$

$$\text{At } Z^*=100\quad \frac{\partial u^*}{\partial z^*}=\frac{\partial w^*}{\partial z^*}=\frac{\partial v^*}{\partial z^*}=\frac{\partial}{\partial z^*}\left(\frac{\partial T^*}{\partial z^*}\right)=0 \tag{9}$$

The governing partial differential equations and boundary conditions are written in dimensionless form according to dimensionless variables deducted from the reference values D, v_0 and ΔT :

$$r^*=\frac{\mathrm{r}}{\mathrm{D_h}},\ Z=\frac{\mathrm{z}}{\mathrm{D_h}},\ u=\frac{\mathrm{u}}{\mathrm{v_0}}^*,\ v^*=\frac{\mathrm{v}}{\mathrm{v_0}},\ w^*=\frac{\mathrm{w}}{\mathrm{v_0}},\ t^*=\frac{\mathrm{v_0}\,t}{\mathrm{D_h}}$$

$$p^*=\frac{p}{\rho_{\mathrm{nf}}\mathrm{V_0^2}}\ ,\quad \mathrm{T}^*=\frac{(\mathrm{T}-\mathrm{T_0})}{\Delta T}\ ,\quad \Delta T=\frac{q_w D_h}{k_{nf}}$$

The dimensionless groups in the governing equations are the well-known numbers of Reynolds (Re) and Prandtl (Pr).

$$\mathrm{Re}=\frac{\rho_f\,\mathrm{v_0}\,D_h}{\mu_{\mathrm{f}}}\ ,\quad \mathrm{Pr}=\frac{\nu_f}{\alpha_f}$$

In order to estimate the heat transfer characteristics, we have calculated local Nusselt number Nu (z^*, θ) and the overall mean Nusselt number $\mathrm{Nu_{av}}$ as:

$$Nu\left(\theta,z^*\right)=\frac{K_{nf}}{K_f}\frac{\left(\partial T^*/\partial r^*\right)\Big|_{r^*=1}}{T^*\left(1,\theta,z^*\right)-T_b^*\left(z^*\right)} \tag{10}$$

$$Nu_{av}=\frac{1}{2\pi L}\int_0^{2\pi}Nu(\theta,Z^*)d\theta dZ^* \tag{10}$$

Where T_b^* is the bulk temperature defined as:

$$T_b^*(z^*)=\frac{\int_{0.5}^{1}\int_0^{2\pi}v^*(r^*,\theta,z^*)T^*(r^*,\theta,z^*)r^*dr^*d\theta}{\int_{0.5}^{1}\int_0^{2\pi}v^*(r^*,\theta,z^*)r^*dr^*d\theta} \tag{11}$$

G. Nanofluid Thermal Properties:

The density, the heat capacitance, the thermal conductivity for Hamilton-Crosser model [3] and the thermal expansion coefficient of nanofluid can be determined as follows:
The density of the nanofluid is given by:

$$\rho_{nf}=(1-\phi)\rho_f+\phi\rho_s \tag{12}$$

$$(\rho Cp)_{nf}=(1-\varphi)(\rho Cp)_f+\varphi(\rho Cp)_s \tag{13}$$

$$k_{nf}=\left(\frac{k_s+(n-1)k_f-(n-1)\phi(k_f-k_s)}{k_s+(n-1)k_f+\phi(k_f-k_s)}\right)k_f \tag{14}$$

Or n =3 for spherical nanoparticles.

TABLE I. SPHERICITY Ψ FOR DIFFERENT SHAPES NANOPARTICLES

Model	Platelet	Blade	Cylinder	Brick
ψ	0.52	0.36	0.62	0.81

The viscosity of the nanofluid can be calculated using the [9] formula as:

$$\mu_{nf}=\mu_f(1+a\phi+b\phi^2) \tag{15}$$

Dynamic viscosity is used, being valid for both spherical and non-spherical shapes nanoparticles according to this model [9], Where ***a*** and ***b*** are constants and depend on the particle shape as given in Table 2.

TABLE II. CONSTANTS EMPIRICAL SHAPE FACTORS

Model	Platelet	Blade	Cylinder	Brick
a	37.1	14.6	13.5	1.9
b	612.6	123.3	904.4	471.4

$$(\rho\beta)_{nf}=\left[\frac{1}{1+\frac{(1-\phi)\rho_f}{\phi\rho_s}}\frac{\beta_s}{\beta_f}+\frac{1}{1+\frac{\phi}{(1-\phi)}\frac{\rho_f}{\rho_f}}\right]\beta_f \tag{16}$$

The thermophysical properties of water and nanoparticles are shown in Table 3.

TABLE III. THERMOPHYSICAL PROPERTIES OF WATER AND NANOPARTICLES

PROPERTIES	***Water***	***Ag***	***CuO***
$\rho(kgm^{-3})$	997.1	10500	540
Cp (J $Kg^{-1}K^{-1}$)	4179	235	6500
$k(Wm^{-1}K^{-1})$	0.613	429	18.0
$\mu\ (m^2s^{-1})\times10^{-3}$	0.855	-	-

III. GRID INDEPENDENCY AND CODE VALIDATION

The dimensionless governing equations were solved by using the finite volume method developed by [10] and the SIMPLER algorithm with a second order precision. The convective and nonlinear terms have been discretized according to the Adams-Bashforth numerical scheme and the fully implicit scheme for the diffusive and pressure terms. For the spatial discretization, we used the second order central differences. Regular grids are used in this study and the mesh size is in increased from 26×34×112 to 52×64×162 shows the variations of the axial Nusselt number show in Fig. 2, for the control parameter for Re=600, Pr=6.2 for pure water. The selected grid for the present calculation consisted of 44, 52 and 162 nodes, in the radial, circumferential and axial directions respectively. The average Nusselt number with the grid number is given in Table 4.

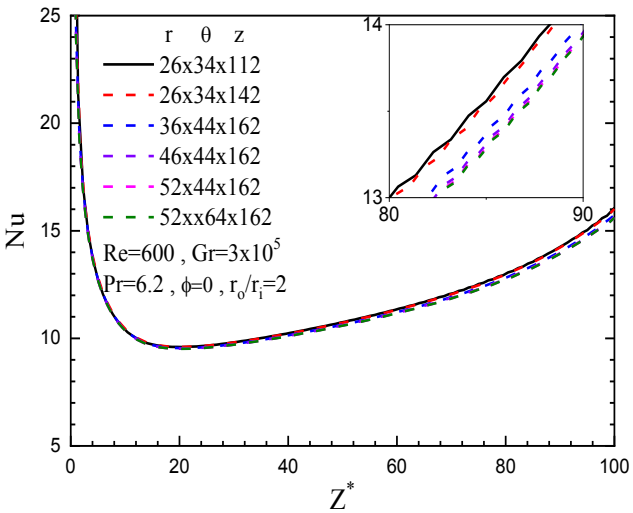

Figure 1: (a), (b) Grid independence tests

TABLE IV. EFFECT OF THE GRID TESTING

Mesh	Grid Size	$Nu_{average}$	$\frac{Nu_{large\ grid} - Nu_{small\ grid}}{Nu_{large\ grid}}$
M1	26×34×112	12.035	-
M2	26×34×142	12.026	-7.48378×10^{-4}
M3	36×44×162	11.90	-1.0588×10^{-2}
M4	46×44×162	11.86	-3.3727×10^{-3}
M5	52×44×162	11.85	-8.4388×10^{-4}
M6	52×64×162	11.84	-8.4459×10^{-4}

Concerning the validation of the code, Fig.3 shows the variation of the local Nusselt number versus the dimensionless length (x/D). In the present results have been compared with experimental data of [11] numerical results of [12], Shah equation [13] and classical theory. The results show good agreement with experimental data and numerical results. The results show good agreement.

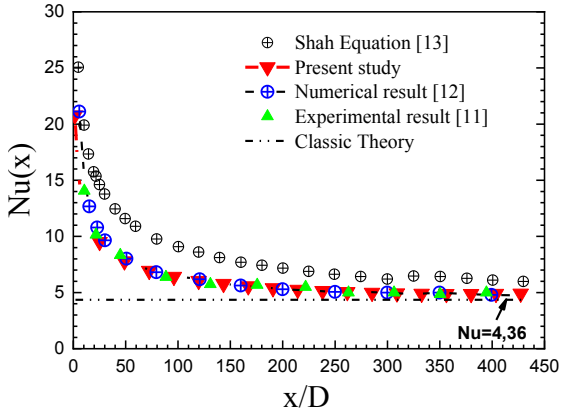

Figure 2: Comparison of the computed local Nusselt number values with the experimental data, numerical results and empirical equations for pure water

IV. RESULTS AND DISCUSSION

In this section, we present numerical results for the laminar flow forced convection in a concentric annulus by using two nanoparticles types Ag and CuO with four shapes Blade, Platelet, Cylinder, and Brick. The governing parameters of the heat transfer and fluid flow are as follows: a Reynolds and Grashof numbers Re=800 and Gr=0, nanoparticles volume fraction from 0% to 6%. The effect of particle shapes and types, volume fraction on the bulk and wall temperature profiles, local and average Nusselt number are analyzed and discussed in this section.

A. Dimensionless Temperature Profile:

The bulk and wall temperatures of two nanoparticles shapes and two types Ag and CuO dispersed in water base fluid. Fig. 4 (a,b) shows that the wall temperature and the bulk temperature increase with the increase in the volume fraction, in the other hand the bulk temperature increase linearly along the tube with the increase of volume fraction for blade nanoparticle shape. The effect of the nanoparticles' shapes on the bulk and wall temperature for the blade, platelet, cylinder, and brick, shown in Fig. 5, The figure shows that the average temperature and the walls found with the different geometry of the nanoparticles are different, also finds that the blade shape gives the greatest temperature follow by platelet, cylinder, and brick. Note also that the bulk and wall temperatures obtained using Ag nanoparticles are highest compared with the nanoparticle CuO. This result back to the large thermal conductivity which is characterized by silver nanoparticles (Ag) compared to the thermal conductivity of nanoparticles of copper oxide (CuO).

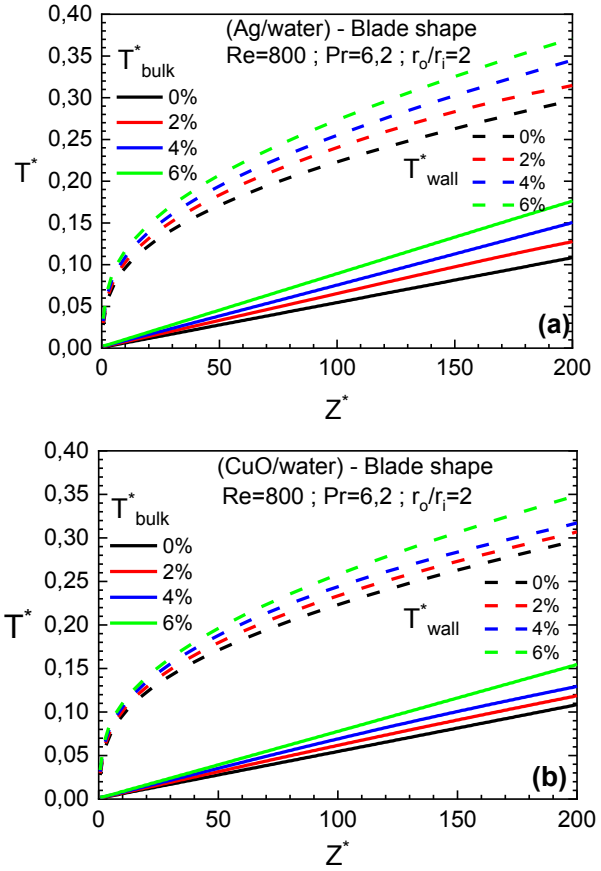

Figure 4: Wall temperature and bulk temperature profile for the nanoparticle blade shape: a) Ag, and b) CuO

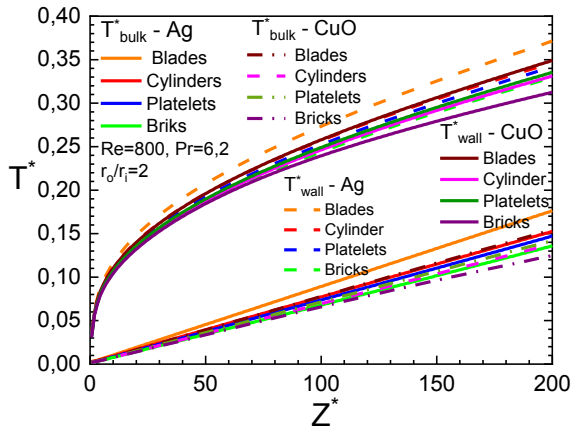

Figure 5: A Comparison of the average temperature and the wall of the two types of nanoparticles and different shapes Ag and CuO for 6% volume fraction

B. Nusselt Number:

Figs. 6(a,b) presents the axial evolution of local Nusselt number on the heated part of the inner wall of the outer cylinder for two nanofluids (A/water) and (CuO/water), four different shapes like blades, cylinders, platelets, and bricks. the highest values of the local Nusselt number are obtained at the inlet of the duct because the thermal boundary layer is a little affected by the secondary flows, after near to z*= 20, the large decrease of the axial Nusselt number is the same for all cases. This is understood because the buoyancy force is very weak in this zone, then from this zone, the Nusselt number remains almost constant along the annulus until the exit.

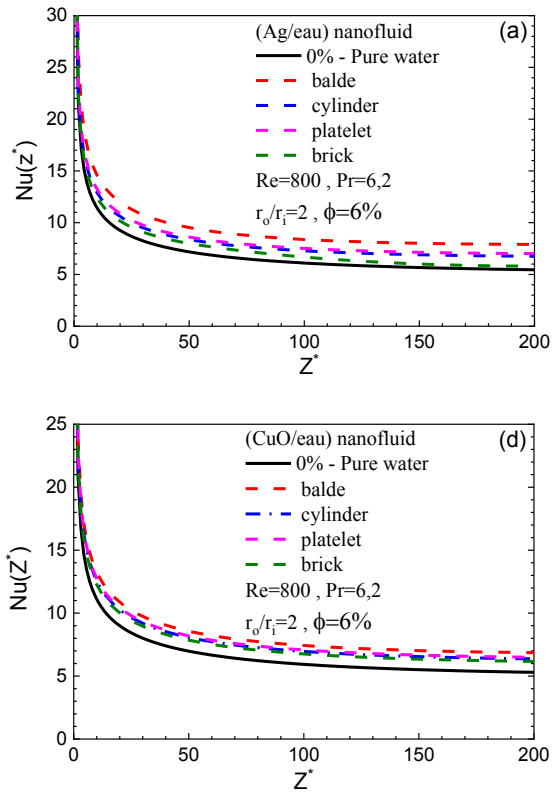

Figure 6: Axial variation of the Nusselt number for Ag/water) and (CuO/water) nanofluids for 6% volume fraction and different nanoparticles shapes

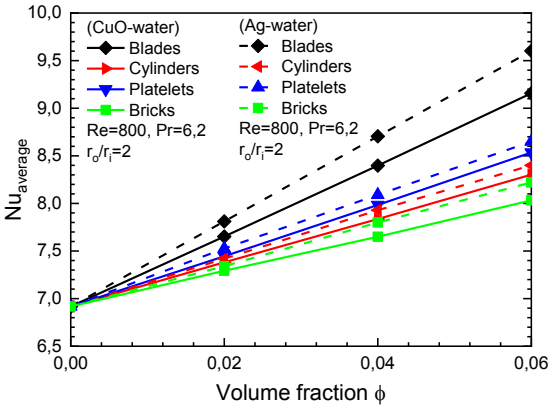

Figure 7: Comparison of the average Nusselt number for different shapes

Fig. 7 illustrates the average Nusselt number of (Ag/water) and (CuO/water), It is clear that the average Nusselt number increases linearly as the volume fraction increases, the higher average Nusselt number to find for the blade nanoparticle shape followed by the platelet and cylinder in the last brick shape. In general, for thermal conductivity of the nanoparticles raising the temperature gradient decreases thus the Nusselt number increases this proves that the nanoparticles of blade shape at the largest Nusselt number this observation obtained for both nanoparticles Ag and CuO.

I. CONCLUSION

In the present numerical study, the finite volume method was employed to analyze the effect of the type and shape of nanoparticles on convective heat transfer in an annular duct with the heated outer cylinder. Some important conclusions from the study are given below:

- The bulk and wall temperatures, the axial and average Nusselt numbers increasing with the increase of the volume fraction.
- The blade shape of the nanoparticle shows maximum values for the temperature and even for the Nusselt number.
- For the same shape of the nanoparticle, Silver (Ag) dispersing in the water base fluid gives better heat transfer than the Copper oxide (CuO).

Nomenclature

Cp specific heat , (J/kg K)
D diameter, (m)
k thermal conductivity, (W/m K)
Nu Nusselt number
L length, (m)
P pressure, (Pa)
Pr Prandtl number
q heat flux, (W/m^2)
Re Reynolds number
T temperature, (K)
r radius, (m)
u radial velocity component, (m/s)
v axial velocity component, (m/s)
w tangential velocity component, (m/s)
z axial direction, (m)

Greek symbols

θ angular coordinate
ϕ volume fraction
μ dynamic viscosity, (kg/m s)

subscripts

b bulk
nf nanofluid
f base fluid
0 inlet condition
s solide
w wall
* dimensionless parameters

REFERENCES

[1] S. U. S. Choi, "Enhancing Thermal Conductivity of Fluids with Nanoparticles, in Development and Applications of Non-Newtonian Flows," ASME FED 231/MD, vol. 66, pp. 99–103, 1995.

[2] S. U. S. Choi and A. Eastman, "Enhancing Thermal Conductivity of Fluids with Nanoparticles," Energy Technology and Materials Science Division Argonne National Lab, 1995.

[3] R. L. Hamilton and O. K. Crosser, "Thermal conductivity of heterogeneous two-component system," I&EC Fundamentals, vol. 1 (3), pp. 187–191, 1962.

[4] J.C. Maxwell, "A Treatise on Electricity and Magnetism," 2nd ed, Oxford University Press, Cambridge, UK, p. 435, 1904.

[5] M. Izadi, A. Behzadmehr, and D. Jalali-Vahida, "Numerical study of developing laminar forced convection of a nanofluid in an annulus," International Journal of Thermal Sciences vol. 48 pp. 2119–2129, 2009.

[6] Reza Mokhtari Moghari, Farhad Talebi, Roohollah Rafee, and Mohammad Shariat, "Numerical Study of Pressure Drop and Thermal Characteristics of Al2O3–Water Nanofluid Flow in Horizontal Annuli," Heat Transfer Engineering, vol. 36(2), pp. 166-177, 2015.

[7] BENKHEDDA Mohamed and BOUFENDI Toufik, "Computational study of the mixed convection heat transfer of Ag-water nanofluid in an annular duct.," in Renewable and Sustainable Energy Conference (IRSEC), International. IEEE, 2016. p. 639-644, 2016.

[8] Mohamed Benkhedda, Toufik Boufendi, and S. Touahri, "Laminar mixed convective heat transfer enhancement by using Ag-TiO2-water hybrid Nanofluid in a heated horizontal annulus," Heat and Mass Transfer, 2018.

[9] Timofeeva E. V, J. L. Routbort, and D. Singh, "Particle shape effects on thermophysical properties of alumina nanofluids," Journal of Applied Physics, vol. 106, p. 014304, 2009.

[10] S. V. Patankar, Numerical Heat Transfer and Fluid Flow. New York: McGraw-Hill, 1980.

[11] D. Kim, Y. Kwon, Y. Cho, C. Li, S. Cheong, Y. Hwang, et al., "Convective heat transfer characteristics of nanofluids under laminar and turbulent flow conditions," Current Applied Physics, vol. 9, pp. e119-e123, 2009.

[12] Javad Bayat and Amir Hossein Nikseresht, "Investigation of the different base fluid effects on the nanofluids heat transfer and pressure drop," Heat Mass Transfer, vol. 47, pp. 1089–1099, 2011.

[13] R. K. Shah and A. L. London, Laminar Flow Forced Convection Heat Transfer and Flow Friction in Straight and Curved Ducts- A Summary of Analytical Solutions. Academic Press, New York, NY, 1971.